DETECTION OF *PHELLINUS NOXIUS* DECAY IN *STERCULIA FOETIDA* TREE

CJ Lin[1, *], CH Chung[1], ML Wu[1] & CL Cho[2]

[1]*Taiwan Forestry Research Institute, 53 Nanhai Road, Taipei 100, Taiwan*
[2]*Department of Natural Resources, National I-Lan University, 1, Sec 1, Shen-Lung Road, Ilan 260, Taiwan*

Received May 2012

LIN CJ, CHUNG CH, WU ML & CHO CL. 2013. Detection of *Phellinus noxius* decay in *Sterculia foetida* tree. The extent and location of decay in a damaged standing hazel bottle tree (*Sterculia foetida*) infected with brown root rot (*Phellinus noxius*) were determined using non-destructive evaluation (NDE) techniques, namely, visual inspection, stress wave tomography, drilling resistance and crushing strength. The stress wave velocity, drilling resistance and crushing strength of the infected tree were lower than those of the uninfected tree. Greater decay and damage as well as weaker strength properties were found near the root and bark of the trunk at the base of the infected tree. Observation in the field showed that decay and wood deterioration due to brown root rot developed from the root upwards to the trunk and from the bark penetrating inwards to the pith. Various NDE techniques can be used in combination to detect decay in living tree infected with brown root rot.

Keywords: Acoustic tomography, root rot, drilling resistance, tree risk, non-destructive evaluation

LIN CJ, CHUNG CH, WU ML & CHO CL. 2013. Pengesanan reput *Phellinus noxius* pada pokok *Sterculia foetida*. Takat dan lokasi reput busuk akar perang (*Phellinus noxius*) pada pokok hidup *Sterculia foetida* dikaji menggunakan teknik penilaian tak musnah (NDE) iaitu pemeriksaan secara pemerhatian, tomografi gelombang tegasan, rintang gerudi dan kekuatan hancur. Nilai halaju gelombang tegasan, rintang gerudi dan kekuatan hancur bagi pokok yang dijangkiti adalah lebih rendah daripada pokok yang sihat. Pereputan dan kerosakan yang lebih teruk serta ciri kekuatan yang lebih lemah didapati berdekatan akar dan kulit batang pada pangkal pokok yang dijangkiti. Pemerhatian di lapangan menunjukkan yang pereputan dan kemerosotan kayu akibat busuk akar perang berkembang ke atas dari akar ke batang dan dari kulit ke empulur. Pelbagai teknik NDE boleh digunakan secara gabungan untuk mengesan reput pada pokok hidup yang dijangkiti busuk akar reput.

INTRODUCTION

Brown root rot (*Phellinus noxius*) is the most important fungal root disease in Taiwan. Brown root rot causes white rot in roots and wood tissues of the basal stem as well as lesions in roots and bark tissues of the basal stem. A decline in symptoms occurs when girdling lesions appear on the basal stem (Ann et al. 2002). Trees infected with brown root rot topple easily with failure occurring at the base of the trunk. Concerns for public safety and urban forest conservation strongly support the development and application of rapid and precise diagnostic techniques to detect decay and other types of structural defects in trees (Wang & Allison 2008).

Standing trees must be evaluated in order to maintain in-situ structural safety. Various non-destructive evaluation (NDE) techniques have been employed to detect decay in trees in order to identify hazardous trees. NDE is the science of identifying physical and mechanical properties of a piece of material without altering its end-use capabilities and then using this information to make decisions regarding appropriate applications (Pellerin & Ross 2002). Visual tree assessment includes visual inspection of the tree to look for external evidence of internal defects, instrumental measurements of internal defects and evaluation of the residual strength of the wood (Mattheck & Breloer 1994). Arboriculturists consider visual tree assessment an essential practice, which serves as the starting point for evaluating tree defects and providing basic information of tree growth performance and stability. Stress and ultrasonic wave

**d88625002@yahoo.com.tw*

evaluation measurements of wood have proven to be effective parameters for detecting and estimating deterioration in tree stem and wood structure (Lin et al. 2000, Pellerin & Ross 2002). X-ray, computed tomography technique and magnetic resonance imaging are reliable imaging approaches to evaluating internal characteristics and defects in trees (Bucur 2003, Nicolotti et al. 2003). In recent years, NDE techniques have been developed for tomographic investigations. Acoustic tomographic measurements in wood have been found to be effective in detecting and estimating decay in tree stems (Gilbert & Smiley 2004, Bucur 2005, Wang et al. 2007, Deflorio et al. 2008, Lin et al. 2008, Wang & Allison 2008, Wang et al. 2009).

Acoustic tomography has been proven to be the most effective technique for detecting internal decay, locating the position of defects, and estimating their size, shape and characteristics. A drilling resistance technique can be employed to determine the position and nature of the defect (Wang et al. 2005, 2007, Wang & Allison 2008, Lin et al. 2011). Fractometer is a device that breaks a radial increment core along the direction of the fibre to measure the fracture strength (Chiu et al. 2006, Lin et al. 2007). Many diagnostic devices such as penetrometer (e.g. resistograph), acoustic detector, electrical conductivity meter and fractometer are available for detecting internal decay and other defects in living trees (Larsson et al. 2004).

For both public safety and tree protection, faster, safer, more cost-effective and precise diagnostic NDE techniques have been developed for detecting damage and defect in living trees. These techniques can be used in combination to achieve better accuracy in determining the location and extent of decay. The purpose of the present study was to assess the location and extent of decay in a standing hazel bottle tree (*Sterculia foetida*) infected with brown root rot (*P. noxius*) using various techniques, namely, visual inspection, stress wave tomography, drilling resistance and crushing strength of cored samples.

MATERIALS AND METHODS

The structural stability of two hazel bottle trees located at the Taipei Botanical Garden, Taiwan Forestry Research Institute, Taipei, Taiwan, was evaluated. One tree was infected with brown root rot while the other was not. Comparison was made to study the difference between the decayed and undamaged trees. Both trees were about 20 m tall. The diameter at breast height of the infected tree was 49 cm while that of the undamaged tree was 51 cm. To screen for trunk and root decay, visual inspection was conducted to look for anomalies such as fungal conks, cavities, bulges and root-related problems. Fruiting bodies of brown root rot were observed on the trunk surface at the base (at about 30 cm above ground, Figure 1) and part of the root surface was damaged and showed decay.

Further screening for internal trunk defects using stress wave testing was conducted with a microsecond timer. Multiple stress wave measurements were carried out at eight equidistant points (eight probes) on the trunks. All sensors were located in the trees at about 30 cm above ground and the transducer was connected at an angle of 90° to the trunk axis to detect the propagated travel time and stress wave. The transmitter probe was first positioned at point 1 with a stress wave pulse acquired by the receiver probe at the other seven points. Hammer tapping was made from points 1 to 2, 3, 4, 5, 7 and 8. Measurements were repeated with the transmitter probe positioned at each point, thus giving 28 (for a complete round trip: 7 receiving probes × 8 transmitter probes ÷ 2 [same path was measured twice]) independent propagation time measurements for each investigated section. A complete data matrix was obtained through this measurement process at each test location.

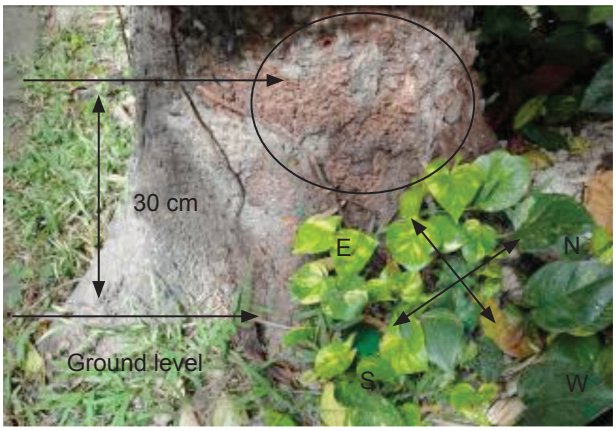

Figure 1 Fungal fruiting bodies of brown root rot on trunk surface at the base of infected tree

The circumference for each cross-section and the distances between sensors were measured using a tape measure. These measurements served as inputs for the system software to map the approximate geometric form of the cross-sections. Firstly, on completing the acoustic measurements, a tomogram was constructed for each cross-section using the ArborSonic software. Secondly, due to differences in species and paths, the two-dimensionel (2D) image was obtained using Arbotom software based on original stress wave transmission times (no adjusted and regularised times) for understanding the experimental values in this study. To quantitatively assess the tomograms, all corresponding stress wave velocities at each pixel of the tomogram were further calculated by visualising and converting the tomograms to yield stress wave velocity maps of the cross-sections.

After the information of stress wave characteristics of each cross-section provided by the tomograms was tabulated, drilling resistance was conducted using a resistograph. The drilling paths ran in the radial direction from the bark to the pith of a trunk cross-section. Sound wood is dense, hard in texture and has high resistance to drill penetration. In contrast, severely decayed wood is less dense, softer in texture and has reduced drilling resistance (Pokorny 1992). Next, 5-mm diameter cores were cut from the trunk and root using an increment borer. A fractometer was used to evaluate the crushing strength of core samples (in green state) in the bark to pith direction at an interval of 6 mm. Figure 2 summarises the steps involved in tree assessment.

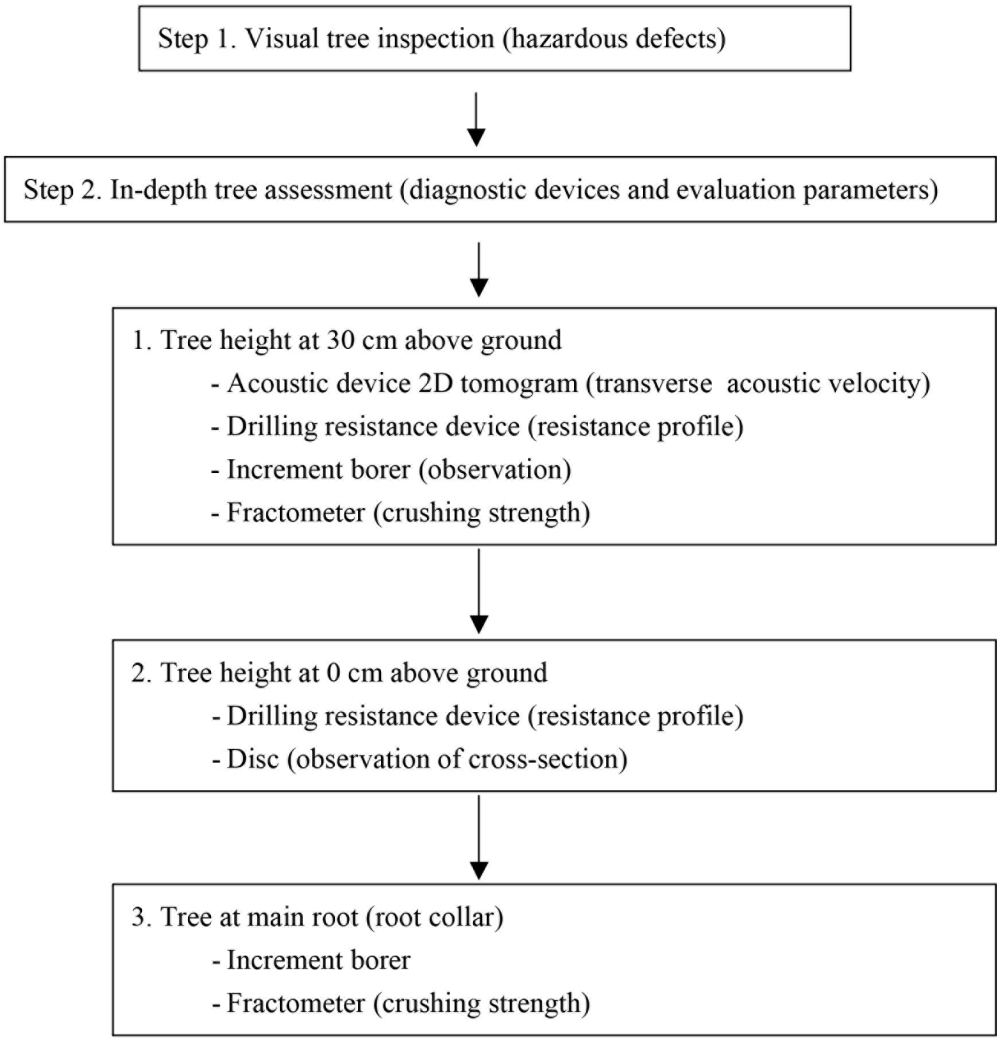

Figure 2 Flowchart of steps involved in tree assessment

RESULTS

Figure 3 displays the 2D tomography and corresponding stress wave velocity (V) values of the undamaged tree. The average V was 1475 (range 1113–1656) m s^{-1}, which served as a reference value for comparison between uninfected (undamaged) and infected (decayed) living trees. Figure 4 shows the 2D tomography and corresponding V values of the infected tree. The average V was 1138 (range 325–1429) m s^{-1}. The infected tree had lower average V and individual stress wave velocities compared with the uninfected tree. As shown in Figure 4, lower transverse stress wave velocities (map grids) were observed in the southern direction of the infected tree, with the damaged area reaching the centre of the cross-section (from bark to pith). However, there was no obvious difference in stress wave velocities of other aspects between the core and periphery of the trunk.

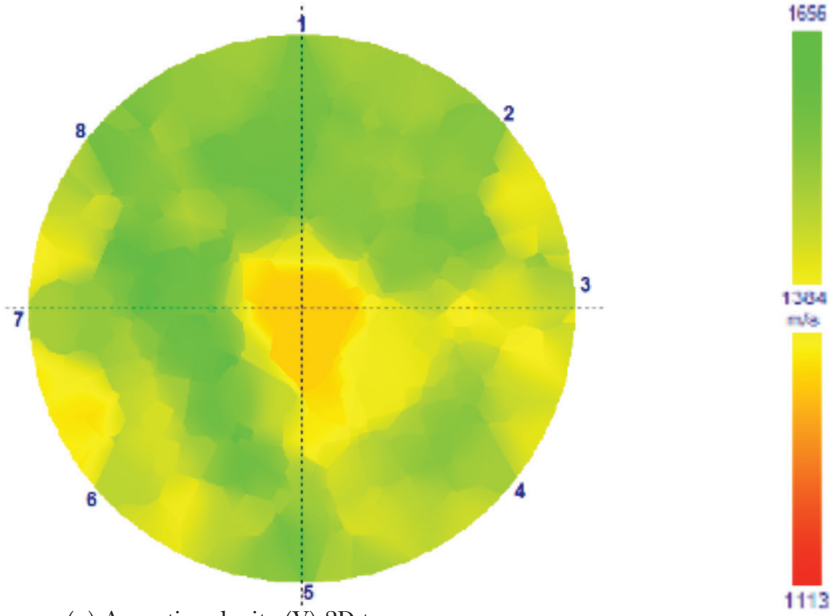

(a) Acoustic velocity (V) 2D tomogram

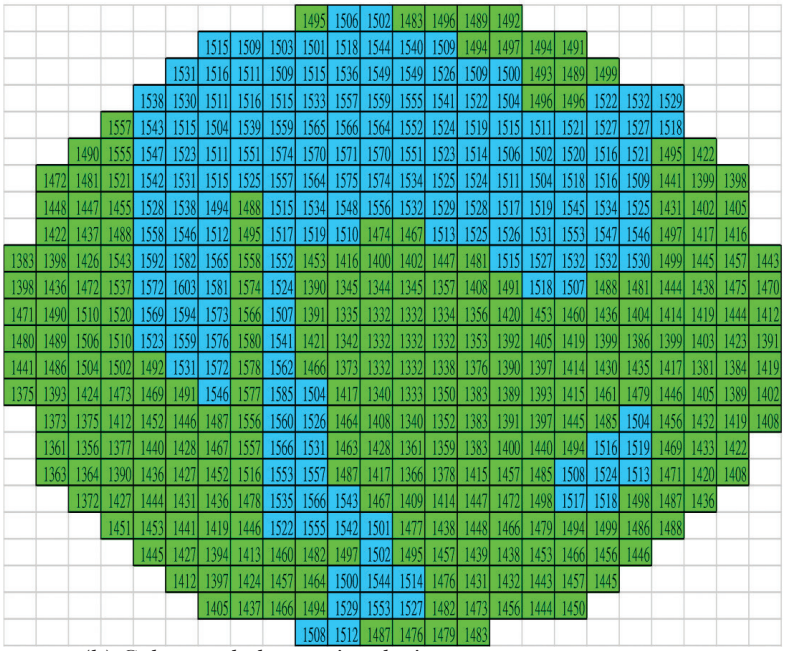

Colour coded green, V < 1500 m s^{-1}
Colour coded blue, V ≥ 1500 m s^{-1}

(b) Colour-coded acoustic velocity map

Figure 3 (a) Acoustic tomography (red–yellow–green) and (b) corresponding stress wave velocity map grids (2 cm × 2 cm, adjusted for size) for the uninfected hazel bottle tree (undamaged, at 30 cm above ground)

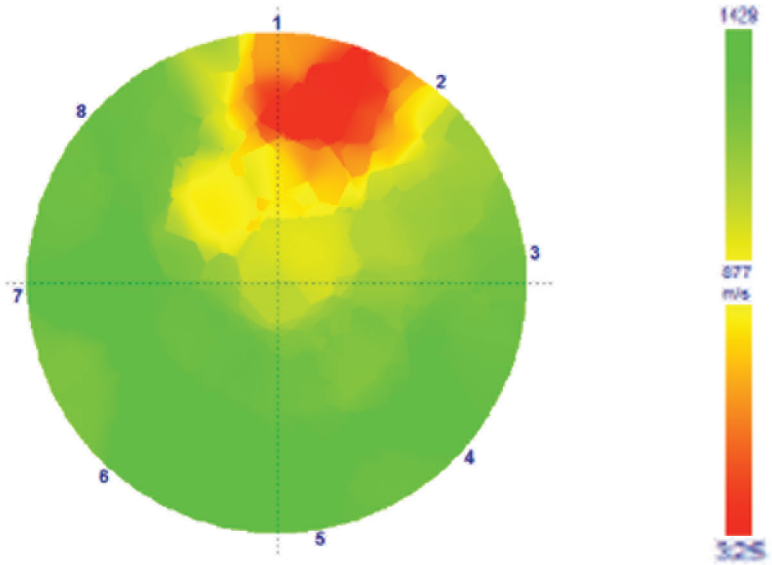

(a) Acoustic velocity (V) 2D tomogram

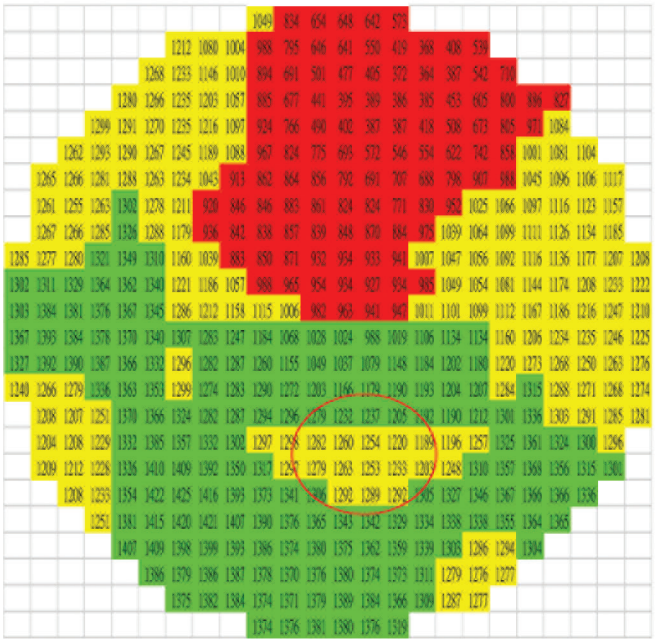

(b) Colour-coded acoustic velocity map

Colour coded red, V < 1000 m s^{-1} serious decay)
Colour coded yellow, 1000 m s^{-1} ≤ V < 1300 m s^{-1}
Colour coded green, V ≥1300 m s^{-1}

Photo of cross-section (southern direction)

Figure 4 (a) Acoustic tomography (red–yellow–green) and (b) corresponding stress wave velocity map grids (2 cm × 2 cm) for the infected hazel bottle tree (decayed, at 30 cm above ground)

The drilling resistance profiles of the uninfected tree at 30 cm above ground are shown in Figure 5. The drilling resistance (R) in the radial direction increased inwards from the periphery to about 2.5 cm from the bark, then decreased to about 5 cm from the bark, and increased again, maintaining more or less the same value in the pith region. The average value of R at 2.5 cm from the bark was 243.3 (241.3, 249.4, 235.9 and 246.6 for the northern, eastern, southern and western directions respectively), which served as a reference value for comparison between undamaged and decayed living trees. The average R value at 5 cm from the bark was 112.1 (112.2, 105.2, 119.5 and 111.6 for the northern, eastern, southern and western directions respectively).

Figure 6 shows the drilling resistance profiles of the tree infected with brown root rot at 30 cm above ground. The average R value of

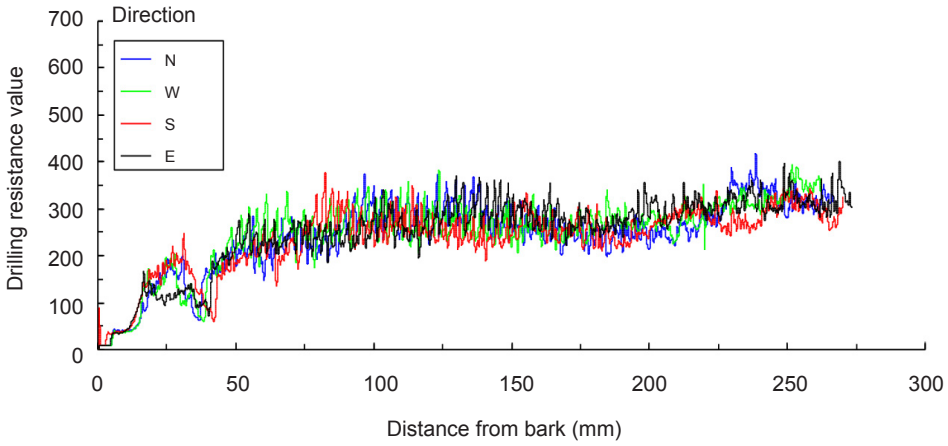

Figure 5 Radial drilling resistance profiles of the uninfected hazel bottle tree (undamaged, at 30 cm above ground)

the entire radial area (from the bark to the pith) was 309.9 while that at 5 cm from the bark was 101.2. In comparison, the average R value for the entire radial area in the infected tree (Figure 6) was larger than that in the uninfected tree, while the average R value at 5 cm from the bark in the decayed tree was lower than that of the undamaged tree (Figure 5). The average R value near the bark of the infected tree was smaller than that of the uninfected tree. The R value in peripheral wood was affected by decay but not that of the internal wood because decay developed from the bark, spreading inwards to the pith of the infected tree (field observation).

Figure 7 shows the drilling resistance profiles of the infected tree at ground level. The average R values of the entire radial area (from the bark to the pith) and at 5 cm from the bark were 222.8 and 81.1 respectively. For the entire radial area and at 5 cm from the bark, the average R values in the decayed tree were smaller than those in the undamaged tree. The R value in peripheral wood was mainly affected by decay. The average R value of the infected tree at ground level was lower than that at 30 cm above ground. Overall, wood decay was more serious at ground level than at 30 cm above ground and more significant for peripheral wood than for internal wood.

Comparison of average radial drilling resistance profiles of the infected and uninfected hazel bottle tree is shown in Figure 8. For the entire radial direction, average R values at the pith of the decayed tree were larger than that in the undamaged tree. Moreover, at 5–6 cm from the bark, average R values in the decayed tree were smaller than those in the undamaged tree (bark thickness of about 25–30 mm).

The uninfected living tree could not be cut down and the infected tree was removed immediately after experiment. So the actual internal state of trunk extracted cores instead of the entire cross-section. After acoustic testing and drilling resistance, cores of 5-mm diameter were cut from the trunk and root by an incremental borer. The presence, size and location of decay in the core samples were determined by visual inspection (Figure 9). Two core samples (cores 1 and 2) of the infected tree which were taken from the roots showed that the roots were decayed near the bark (core 1) and the entire core length (core 2). Three core samples (cores 3, 4 and 5) of the infected tree which were taken from the trunk at 30 cm above ground revealed damaged wood near the pith of the trunk (core 3) and around 4 cm from the bark (cores 3 and 4) as well as about 10 cm from the bark (core 5).

Two core samples (cores 6 and 7) of the undamaged tree which were taken from the trunk at 30 cm above ground showed sound wood from the bark to the pith. The tree infected with brown root rot had greater damage near the root and bark of the trunk at the base.

NDE cannot be used for direct strength measurement. Hence, wood strength must be confirmed by actual inspection. In this study, the crushing strength of core samples was investigated. The average crushing strength of the undamaged tree (core 7) was 16.6 MPa (5–30 MPa), which served as a reference for comparison between uninfected and infected living trees. The average crushing strengths of the infected tree with decay damage at the root (core 2) and at 3 cm from the bark of the trunk (core 3) were 7.5 and 3.0 MPa respectively.

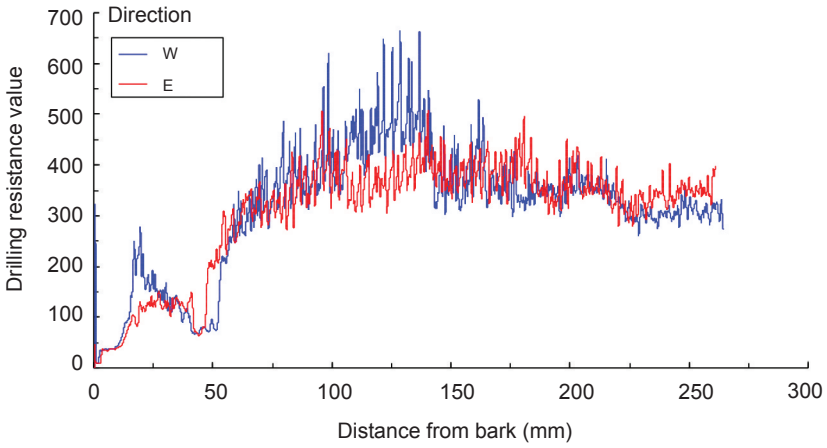

Figure 6 Radial drilling resistance profiles of the infected hazel bottle tree at 30 cm above ground

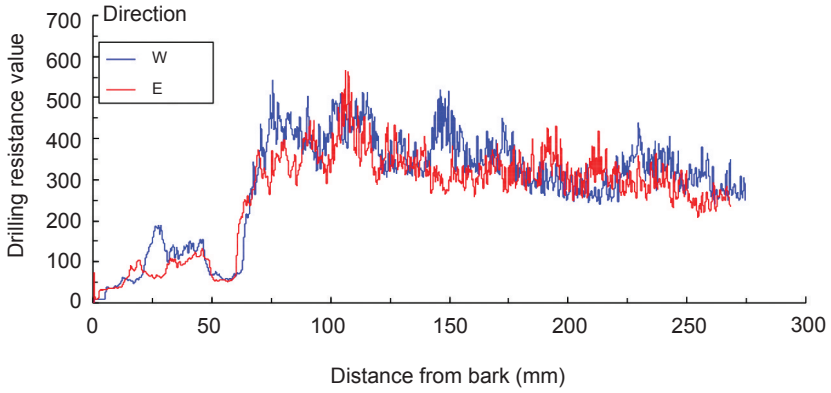

Figure 7 Radial drilling resistance profiles of the infected hazel bottle tree at ground level

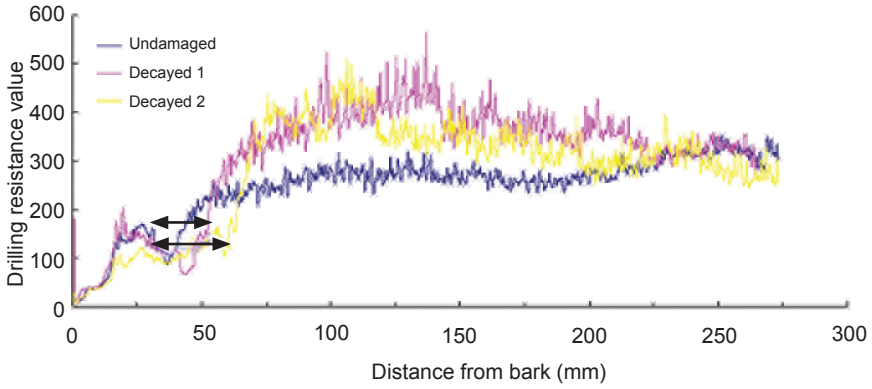

Figure 8 Average radial drilling resistance profiles of the uninfected (undamaged, at 30 cm above ground) and infected (decayed 1 at 30 cm above ground, decayed 2 at ground level) hazel bottle tree; ◄► decayed wood depth (10–30 mm); bark thickness about 25–30 mm

Some measurements could not be made due to serious decay. The tree infected with brown root rot had lower average crushing strength than the undamaged tree. A sharp drop in crushing strength occurred at the root and in the trunk close to the bark.

Finally, the hazel bottle tree infected with brown root rot was felled and discs of 5 cm thick were cut from the trunk at 5 cm above ground. A sampled disc of the tree (southern direction) is shown in Figure 10. Only a quarter of the disc was sampled for visual observation of the

Figure 9 Core samples of infected (decayed) and uninfected (healthy) hazel bottle trees: core 1 = western direction of decayed roots, core 2 = eastern direction of decayed roots, core 3 = eastern direction of the decayed trunk at 30 cm above ground, core 4 = southern direction of the decayed trunk at 30 cm above ground, core 5 = northern direction of the decayed trunk at 30 cm above ground, core 6 = southern direction of the undamaged trunk at 30 cm above ground and core 7 = north-eastern direction of the undamaged trunk at 30 cm above ground

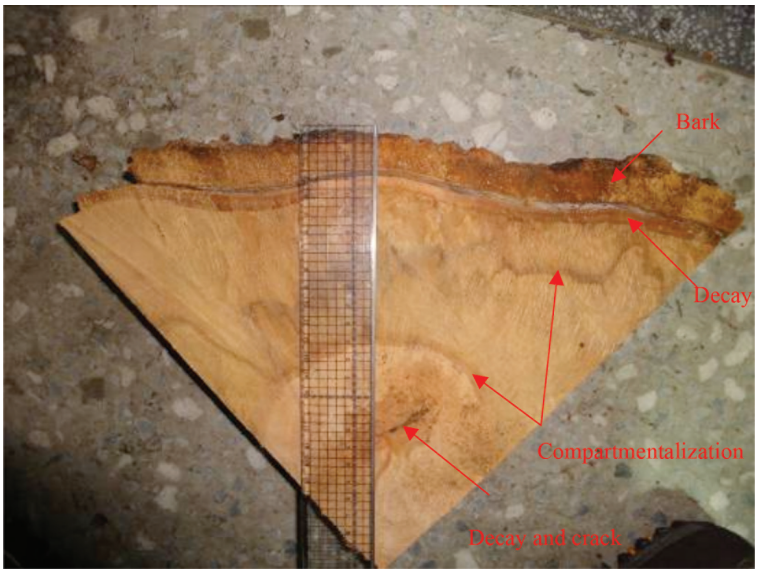

Figure 10 Sampled disc of hazel bottle tree (southern direction) infected with brown root rot

damaged peripheral region and the inner region near the pith. The bark thickness was about 25–30 mm and the radial thickness of decayed peripheral wood in the trunk was about 10 mm. The internal wood near the pith in the trunk showed different grades of deterioration (decay radius about 50 mm). The intermediate wood between peripheral and inner layers of trunk showed evidence of compartmentalisation.

DISCUSSION

In this study, lower transverse stress wave velocities (map grids) were observed in the southern direction of the infected tree. Serious decay and damage reached the centre of the cross-section. In contrast, stress wave velocities of the rest of the other directions between the core and periphery of the trunk showed no obvious

difference (Figure 4). Decay caused by brown root rot occurred in the periphery of the trunk near the bark where stress wave tomography failed to detect efficiently. Severe defects in decayed wood have been reported to reduce the wave velocity to less than 70% of the characteristic values of sound wood (Bethge et al. 1996). In this study, the average V in the undamaged tree was 1475 m s^{-1} with threshold at 1032.5 m s^{-1} (1475 × 0.7 m s^{-1}). However, the average V in the tree infected with brown root rot was 1138 m s^{-1}. The reduction in V is indicative of serious decay, the location and extent of which can be seen in the map grids. The infected tree had lower average and individual stress wave velocities compared with the undamaged tree.

Some studies reported that acoustic tomography could not precisely evaluate the extent and location of decay or the type of defect (Gilbert & Smiley 2004, Wang et al. 2007, 2009, Lin et al. 2011). For example, acoustical tomography underestimates the internal decay and overestimates that in the periphery of the trunk. Acoustical measurements serve mainly to give a 2D image across the entire cross-section for filtering decay and damage, while drilling resistance is required to detect the location and pattern of deterioration. Furthermore, drilling resistance properties can be affected by the cell type, ring structure, moisture content and chemical components. Therefore, to make better assessments of internal conditions and decay of trees, other more effective methods (visual drawing of increment core, drilling resistance and use of fractometer) should also be adopted in combination to enhance the accuracy of the information.

With regard to the higher drilling resistance of internal trunk (heartwood) in the tree infected with brown root rot (Figure 8), Shigo (1989) reported that compartmentalisation of decay and other defects occurred in trees, explaining how wounded trees set boundaries which limited the spread of decay. Pokorny (1992) attributed the preservation of the mechanical strength of a tree to the process of compartmentalisation, which prevented a decaying tree from further deterioration. Compartmentalisation also occurs when wounded trees are infected with canker-causing fungi, mining or boring insects and other agents. In this study, visual inspection revealed compartmentalisation in the intermediate wood between the peripheral and internal layers (Figure 10).

In-depth tree assessments are warranted when a tree poses a high degree of risk to public safety and exhibits defects that cannot be fully evaluated by visual inspection (Pokorny 1992). However, the increment borer and drilling resistance methods are microdestructive assessment approaches (minimally invasive techniques). When a drill destroys the compartmentalisation zone, it opens an access for fungal attack and thus shortens the tree life. In trees already having internal decay, the use of an increment borer and resistograph drilling can break an existing barrier zone within the tree and allows decay to spread into healthy wood. Therefore, when using decay detection devices, the number of drill holes or sensor sites for collecting the required critical field data should be kept to a minimum (Wang et al. 2007).

In this study, decayed wood (weaker strength properties) was found near the root and bark of the infected tree. Infection of brown root rot generally begins from the root system spreading upwards (from the root to the trunk) and from the bark penetrating inwards (from the exterior to the interior). Field observation shows that trees infected with brown root rot do not topple easily but the position of failure is often found in the trunk at the base. In this study, fungal fruiting bodies of brown root rot were observed on the trunk surface at the base. As pointed out by Pokorny (1992), fungal fruiting bodies indicate advanced decay.

Core 3 in this study showed internal (near the pith) decay (Figure 9) in the southern direction of the trunk in the infected tree. This result was in accordance with the corresponding acoustic tomography values displayed in Figure 4, which showed a significant drop in V in the northern direction. Actual symptoms of serious decay (lower acoustic velocities) were observed in the southern direction (from bark to pith) of the cross-section in the infected tree. Infection with brown root rot near the root and bark of the trunk at the base resulted in weakened strength properties in the tree.

Crushing strength is a direct measurement of strength made by the fractometer. However, wood strength is just one component in the overall tree risk assessment. Comparison should be made with standard values of decay free samples of

different tree species. It is recommended that a thorough hazardous tree assessment should include visual inspection of the tree for external evidence of internal defects (e.g. fungal fruiting bodies at the trunk), instrumental measurements of internal defects (e.g. acoustic tomography and drilling resistance methods) and an evaluation of the residual strength of the wood (measured by the fractometer).

REFERENCES

Ann PJ, Chang TT & Ko WH. 2002. *Phellinus noxius* brown root rot of fruit and ornamental trees in Taiwan. *Plant Disease* 86: 820–826.

Bethge K, Mattheck C & Hunger E. 1996. Equipment for detection and evaluation of incipient decay in trees. *Journal of Arboriculture* 20: 13–37.

Bucur V. 2003. *Nondestructive Characterization and Imaging of Wood*. Spring-Verlag Berlin, Heidelberg.

Bucur V. 2005. Ultrasonic techniques for nondestructive testing of standing trees. *Ultrasonics* 43: 237–239.

Chiu CM, Wang SY, Lin CJ, Yang TH & Jane MC. 2006. Application of the fractometer for crushing strength: juvenile-mature wood demarcation in taiwania (*Taiwania cryptomerioides*). *Journal of Wood Science* 52: 9–14.

Deflorio G, Fink S & Schwarze FWM. 2008. Detection of incipient decay in tree stems with sonic tomography after wounding and fungal inoculation. *Wood Science and Technology* 42: 117–132.

Gilbert E & Smiley ET. 2004. Picus sonic tomography for the quantification of decay in white oak (*Quercus alba*) and hickory (*Carya* spp.). *Journal of Arboriculture* 30: 277–281.

Larsson B, Bengtsson B & Gustafsson M. 2004. Nondestructive detection of decay in living trees. *Tree Physiology* 24: 853–858.

Lin CJ, Chang TT, Juan MY & Lin TT. 2011. Detecting deterioration in royal palm (*Roystonea regia*) using ultrasonic tomographic and resistance microdrilling techniques. *Journal of Tropical Forest Science* 23: 260–270.

Lin CJ, Chiu CM & Wang SY. 2000. Application of ultrasound in detecting wood decay in squirrel-damaged standing trees of Luanta China fir. *Taiwan Journal of Forest Science* 15: 267–279.

Lin CJ, Kao YC, Lin TT, Tsai MJ, Wang SY, Lin LD, Wang YN & Chan MH. 2008. Application of an ultrasonic tomographic technique for detecting defects in standing trees. *International Biodeterioration and Biodegradation* 43: 237–239.

Lin CJ, Wang SY & Chiu CM. 2007. Crushing strength sampling with minimal damage to taiwania (*Taiwania cryptomerioides*) using a fractometer. *Wood and Fiber Science* 39: 39–47.

Mattheck C & Breloer H. 1994. Field guide for visual tree assessment (VTA). *Journal of Arboricultural* 18: 1–23.

Nicolotti G, Socco LV, Martinis R, Godio A & Sambuelli L. 2003. Application and comparison of three tomographic techniques for detection of decay in trees. *Journal of Arboricultural* 29: 66–78.

Pellerin RF & Ross RJ. 2002. *Nondestructive Evaluation of Wood*. Forest Products Society, Madison.

Pokorny JD. 1992. *Urban Tree Risk Management: A Community Guide to Program Design and Implementation*. USDA Forest Service Northeastern Area State and Private Forestry, St. Paul.

Shigo AL. 1989. *Tree Pruning: A Worldwide Photo Guide*. Shigo and Trees Associates, Durham.

Wang X & Allison RB. 2008. Decay detection in red oak trees using a combination of visual inspection, acoustic testing, and resistance microdrilling. *Arboriculture and Urban Forestry* 34: 1–4.

Wang X, Allison RB, Wang L & Ross RJ. 2007. *Acoustic Tomography for Decay Detection in Red Oak Trees*. Research Paper FPL-RP-642. US Department of Agriculture, Madison.

Wang X, Wiedenbeck J & Liang S. 2009. Acoustic tomography for decay detection in black cherry trees. *Wood and Fiber Science* 41: 127–137.

Wang X, Wiedenbeck J, Ross Rj, Forsman JW, Erickson JR, Pilon C & Brashaw B. 2005. *Nondestructive Evaluation of Incipient Decay in Hardwood Logs*. General Technical Report FPL-GTR-162. US Department of Agriculture, Madison.

